DOI: 10.1557/adv.2018.648


# Size Effect on the Strength and Deformation Behavior of Glassy Carbon Nanopillars

Almut Albiez[1] and Ruth Schwaiger[1]

[1]*Institute for Applied Materials (IAM), Karlsruhe Institute of Technology (KIT), P.O. Box 3640, 76021 Karlsruhe, Germany*

Corresponding author: Ruth Schwaiger, e-mail: ruth.schwaiger@kit.edu

*ABSTRACT*

*Glassy carbon nanolattices can exhibit very high strength-to-weight ratios as a consequence of their small size and the material properties of the constituent material. Such nanolattices can be fabricated by pyrolysis of polymeric microlattices. To further elucidate the influence of the mechanical size effect of the constituent material, compression tests of glassy carbon nanopillars with varying sizes were performed. Depending on the specific initial polymer material and the nanopillar size, varying mechanical properties were observed. Small nanopillars exhibited elastic-plastic deformation before failure initiation. Moreover, for smaller nanopillars higher strength values were observed than for larger ones, which might be related to smaller defects and a lower defect concentration in the material.*

## INTRODUCTION

Glassy carbon nanolattices can be derived from polymeric photoresists by a pyrolysis process in the absence of oxygen [1-4]. High strength and hardness [5] as well as Young's modulus in the range of 15–40 GPa [1, 4-7] have been reported for glassy carbon, together with a low density (1.3–1.55 g/cm$^3$) as a consequence of the porous structure [4-6]. The combination of these material properties makes glassy carbon an excellent candidate for high-strength low-weight microlattices. It has already been demonstrated that glassy carbon nanolattices exhibit outstanding strength-to-weight ratios and increasing strength with decreasing lattice size [1]. These increasing strength values might be related to both, structural size effects of the nanolattice as well as material size effects of the constituent material.

In this paper, we report compression tests of differently sized glassy carbon nanopillars to analyze the material size effect on the mechanical properties of glassy carbon, which is in addition to structural size effects an important factor contributing to the extraordinary strength of nanolattices. The smaller pillars exhibit higher strength and ductility values, which are affected by the initial polymeric material.

## EXPERIMENTS

Glassy carbon nanopillars with varying heights and diameters were fabricated. The fabrication process consists of two steps, i.e. 3D direct laser writing (3D-DLW; Photonic Professional, Nanoscribe GmbH) of polymeric micropillars on a silicon wafer with the proprietary resist IP-Dip (Nanoscribe GmbH), followed by a pyrolysis process of the polymeric micropillars at 900 °C in a vacuum tube furnace. Details about the pyrolysis processes can be found elsewhere [1]. To ensure adhesion between the pillars and the silicon wafer, especially during pyrolysis, a thin circular pedestal was written on the wafer with a larger diameter than the pillar diameter. Then, the pillar was written on top of the pedestal. The diameters of the polymeric micropillars were varied between 3 µm and 60 µm. Three different sets of pillars (referred to as set (1), (2), and (3)) were produced following the same process steps but using two different resist batches of IP-Dip. The same resist was used for sets (2) and (3), while set (1) was written with a different one. Furthermore, the polymeric pillars of set (1) and set (2) after 3D-DLW had an aspect ratio of 3, while the pillars of set (3) had an aspect ratio of 4.

After pyrolysis, the resulting glassy carbon nanopillars were mechanically characterized by compression testing using a nanoindenter system (G200 XP, Agilent/Keysight Technologies, Inc., now: KLA-Tencor Corporation) equipped with a diamond flat punch of 50 µm in diameter at a strain rate of 0.003 $s^{-1}$. The compression experiment comprised two individual cycles, while the unloading between the two steps was set to 10 % of the maximum load of the first loading cycle. The maximum displacement of the first cycle was set to 1/3 of the displacement of the second cycle. Different maximum displacements were applied to test the pillars under three different loading conditions: linear-elastic, elastic-plastic, and deformation to failure of the pillar. Thermal drift was accounted for during the analysis. The displacement of the glassy carbon nanopillars was determined based on the work of Sneddon [8] following the procedure of Fei *et al.* [9]. A deformation of the diamond indenter tip was not taken into account. For the silicon wafer, a Poisson ratio of 0.28 and Young's modulus of 130 GPa were assumed [10-11]. Stress-strain curves were generated based on the pillar diameter at half height of the nanopillars, which exhibited a very small taper (≤1°), resulting in small differences between pillar diameters at the top and at half height of the pillar. Young's modulus was calculated using the first 5–25 % of the unloading curve of the compression test. The compressive strength of the nanopillars is defined as the maximum stress value within the experiment. After compression testing the pillars were imaged using a helium ion microscope (HIM; ORION NanoFab, Carl Zeiss Microscopy GmbH). The glassy carbon was analyzed by Raman spectroscopy (Horiba Labram HR800, He-Ne Laser with 633 nm).

## RESULTS AND DISCUSSION

During pyrolysis, the polymeric micropillars are thermally decomposed resulting in glassy carbon nanopillars with considerably smaller dimensions and smooth surfaces showing no indication of surface defects. The pillars shrank to ~17–29 % of their original size. Generally, the smaller the size of the polymeric pillar, the more pronounced the shrinkage during pyrolysis, as also observed for glassy carbon

nanostructures made of SU-8 [2]. In our study, the amount of shrinkage was not only dependent on the size of the polymeric micropillar, but also on the batch of IP-DIP that was used for 3D-DLW. The pillars of set (1) showed uniform shrinkage in both height and diameter, whereas for the case of sets (2) and (3) the shrinkage of the height was more pronounced in comparison to the diameter. Consequently, the resulting height-to-diameter ratios of the pillars after pyrolysis varied for the three different pillar sets with ~3.0 for set (1), ~2.3 for set (2), and ~3.3 for set (3). The pedestals, which had been written prior to the polymeric micropillars (compare section "Experiments") transformed into nanolayers, whose thickness could no longer be determined by high resolution microscopy. Finite element (FE) simulations (not shown here) did not reveal any influence of such a nanolayer on the evaluation of the mechanical properties of the glassy carbon nanopillars. Stress-strain curves of differently sized glassy carbon nanopillars of set (3) are shown in figure 1.

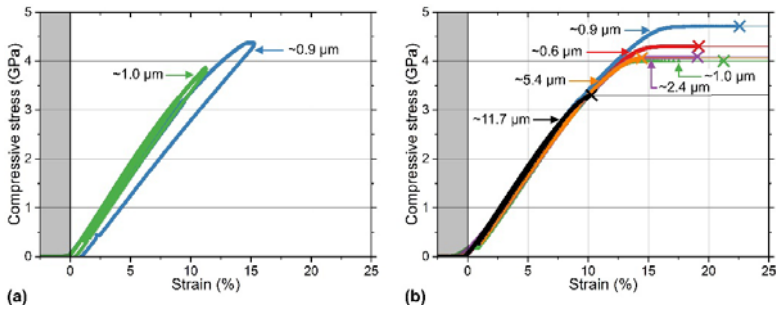


**Figure 1.** Representative compressive stress-strain curves (set (3)) of differently sized glassy carbon nanopillars. The denoted values correspond to the pillar diameter at half height of the pillar. The grey shaded area for negative strain values reflects slight misalignment between the indenter tip and the pillar surface or roughness effects, which shows as nonlinear behavior. In (a) two curves of nanopillars showing elastic-plastic deformation are shown, in (b) the nanopillars were loaded until fracture occurred. Failure of the nanopillars is highlighted by crosses in the stress-strain curves.

Some nanopillars exhibited elastic-plastic deformation behavior as shown in figure 1(a). However, HIM analysis of the deformed pillars (figure 2(a)) does not resolve any shape change due to the plastic deformation, which can be expected since the plastic strain is ≤1 % resulting in a change of the pillar height of only ~35 nm.

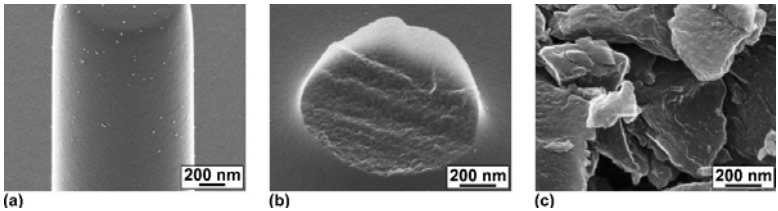


**Figure 2.** HIM images of tested glassy carbon nanopillars of set (3). (a) Shows a close-up view of a plastically deformed nanopillar with diameter ~1.0 µm. The plastic deformation cannot be identified in the HIM image. In (b) and (c) fractured nanopillars are shown with diameters at half height of (b) ~0.9 µm and (c) ~5.4 µm. The morphology of the fracture surface in (b) and of the surface of the debris in (c) is comparable for both pillars.

Elastic-plastic deformation of the small pillars (~0.6 µm – ~2.4 µm diameter) is followed by brittle fracture at strain values of up to ~22 %, as can be seen in figure 1(b) (the points of failure are marked with crosses). This observation is remarkable since failure strains of ≤5 % [12-13] and brittle fracture after linear-elastic behavior [1] has been reported for glassy carbon. Larger pillars (~5.4 µm, ~11.7 µm diameter) exhibit linear-elastic deformation followed directly by brittle fracture (figure 1(b)). Furthermore, smaller pillars reach higher strength values in comparison to larger pillars. The largest pillar (~11.7 µm) reaches a significantly lower compressive strength than the other ones. The fracture surfaces of differently sized nanopillars, which exhibited diverging deformation behaviors prior to failure, show a similar morphology, though, as shown in figures 2(b) and (c). This observation indicates a comparable failure mechanism for these nanopillars, despite the different deformation behaviors.

Mean values of Young's modulus and of the compressive strength as function of the pillar diameter are shown in figure 3 for the three different pillar sets. Here, the mean values of set (3) are indicated by pink symbols and also comprise the experiments shown in figure 1.

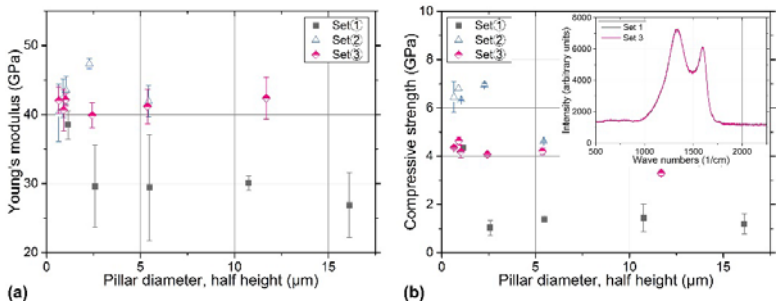


**Figure 3.** (a) Young's modulus and (b) compressive strength of glassy carbon nanopillars as function of pillar diameter at half height of the pillar. Young's modulus was calculated based on the pillar top diameter due to the higher stresses at this location. The results of all three pillar sets are depicted. The inset figure in (b) shows Raman spectra of two pillars of sets (1) and (3), respectively, written with two different resist batches. Error bars represent the standard deviations of at least three (Young's modulus) or two (compressive strength) measurements. For set (1), diameter ~1.1 µm and set (2), diameter ~0.9 µm only one experiment each was performed to determine the compressive strength. The height-to-diameter ratio differs for the three sets. It is ~3.0 for set (1), ~2.3 for set (2), and ~3.3 for set (3).

The values of Young's modulus are in the range of 27–47 GPa and, thus, relatively high in comparison to the majority of literature values of glassy carbon, which are in the range of 15–30 GPa [1, 5-7]. However, also higher values reaching 45 GPa [14] and 62 GPa [12] were reported. Here, the values of Young's modulus strongly depend on the pillar set and, thus, on the batch of IP-Dip that was used. Set (1) shows lower values for large pillars (~29 GPa) and a higher value for the smallest pillar (~39 GPa), whereas sets (2) and (3) show comparable and constant values in the range of ~42 GPa. Apparently the material properties of the glassy carbon depend on the properties of the specific IP-Dip, which is also reflected in the varying shrinkage behaviors of the different resist batches. A dependence of the properties of glassy carbon on the initial material has also been described in the literature; varying carbon contents [3, 13] as well as different mechanical properties [13] of the glassy carbon were reported. However, the Raman spectra of our nanopillars made from different resist batches exhibit

a very similar shape (inset of figure 3(b)), thus, suggesting comparable carbon bond configurations. The actual difference of the materials resulting from different resist batches could not yet be determined.

The compressive strength values of glassy carbon nanopillars (figure 3(b)) show a dependence on the resist batch as well as on the size and the aspect ratio. The nanopillars of set (1) exhibited lower values in comparison to sets (2) and (3), which can be rationalized by the application of the different resist batches. However, for the smallest pillar size of set (1), a strength value comparable to set (3) was achieved (note dark square symbol in figure 3(b) at ~1.1 µm pillar diameter). In general, for all three pillar sets the strength values were observed to increase for the smaller pillar diameters, which indicates an influence of the mechanical size effect, as also observed for, e.g., thin alumina layers [15]. The critical strength of brittle materials depends on the defect size within the material [16]. Gao *et al.* [17] suggest that the defect size scales with the sample size and, thus, decreasing sample sizes result in higher critical strength values. This prediction can explain the increasing strength values of the smaller nanopillars observed in our study. Strength values of glassy carbon depending on the sample size have also been reported in the literature and are related to the concentration [13, 18] and the size [18-19] of defects in the material. A change of the failure mechanism has not been suggested [13], though, as also indicated here by the fracture surfaces of differently sized nanopillars (figures 2(b) and 2(c)) showing comparable features.

With decreasing pillar diameter, the surface-to-volume ratio of the nanopillars increases. As a consequence of the larger surface-to-volume ratio, gases may escape more easily during pyrolysis, resulting in a lower amount of internal defects [13, 18]. Furthermore, small samples might possess a lower concentration of surface defects due to a higher surface tension, which can stand a higher internal gas pressure [18]. By comparing compressive strength values of sets (2) and (3) (which were fabricated from the same resist batch) it can be observed that a lower aspect ratio results in higher strength values (set (2)). An influence of the stress state is unlikely and also our FE calculations (not shown here) do not suggest different distributions of the *von Mises* stress or the triaxiality factor (calculated as the ratio of hydrostatic stress and *von Mises* stress [20]). Nevertheless, the maximum *von Mises* stress determined by FE calculations is higher for the pillars with lower strength values (set (3)). Based on these higher maximum stresses, the material strength might be exceeded at a lower applied stress. The absolute material volume might also affect the strength of the nanopillars. For comparable pillar diameters, the absolute volume of the nanopillars of set (2) is smaller than the volume of the set (3) pillars (by a factor of ~1.4) while the surface-to-volume ratio is higher (by a factor of ~1.1), which might have resulted in smaller defects together with a lower defect concentration.

## CONCLUSIONS

A size effect on the strength and the deformation behavior of glassy carbon nanopillars was identified. Small pillars exhibited elastic-plastic deformation before brittle fracture occurred, whereas the larger pillars exhibited linear-elastic deformation, which was directly followed by brittle fracture. Moreover, smaller pillars reached higher strength values. This might be related to a reduced defect size in combination with a lower defect concentration, as a consequence of smaller absolute volumes and a higher surface-to-volume ratio of smaller nanopillars. While all three pillar sets tested exhibited a mechanical size effect, a strong influence of the initial polymer material on the mechanical properties of the glassy carbon was observed together with a different scaling of the mechanical strength. Despite the identical manufacturing process and the comparable carbon bond configurations, the different modulus and strength levels of the

glassy carbon originating from the different photoresist batches suggest additional compositional and microstructural variations of the pyrolyzed nanopillars.

## ACKNOWLEDGMENTS

We would like to thank Dr. Reiner Mönig (Institute for Applied Materials (IAM), Karlsruhe Institute of Technology (KIT)) for the Raman spectroscopy and the Karlsruhe Nano Micro Facility (KNMF, http://www.knmf.kit.edu) of the Karlsruhe Institute of Technology (KIT) for access to the helium ion microscope at their laboratories.

## REFERENCES

1. J. Bauer, A. Schroer, R. Schwaiger and O. Kraft, *Nat. Mater.* 15, 438-443 (2016).
2. Y. Lim, J.-I. Heo, M. Madou and H. Shin, *Nanoscale Res. Lett.* 8, 492 (2013).
3. A.J. Jacobsen, S. Mahoney, W.B. Carter and S. Nutt, *Carbon* 49, 1025-1032 (2011).
4. S. Sharma, *Materials* 11, 1857 (2018).
5. F.C. Cowlard and J.C. Lewis, *J. Mater. Sci.* 2, 507-512 (1967).
6. O.J.A. Schueller, S.T. Brittain, C. Marzolin and G.M. Whitesides, *Chem. Mater.* 9, 1399-1406 (1997).
7. J.X. Zhao, R.C. Bradt and P.L. Walker Jr., *Carbon* 23, 15-18 (1985).
8. I.N. Sneddon, *Int. J. Eng. Sci.* 3, 47-57 (1965).
9. H. Fei, A. Abraham, N. Chawla and H. Jiang, *J. Appl. Mech.* 79, 061011 (2012).
10. I. Choi, Y. Gan, D. Kaufmann, O. Kraft and R. Schwaiger, *J. Mater. Res.* 27, 2752-2759 (2012).
11. A. Masolin, P.-O. Bouchard, R. Martini and M. Bernacki, *J. Mater. Sci.* 48, 979-988 (2013).
12. M.P. Manoharan, H. Lee, R. Rajagopalan, H.C. Foley and M.A. Haque, *Nanoscale Res. Lett.* 5, 14-19 (2010).
13. G.M. Jenkins and K. Kawamura, *Polymeric carbons - carbon fibre, glass and char*, (Cambridge University Press, Cambridge, 1976) pp. 11-35, 109-134.
14. G.M. Jenkins, K. Kawamura and L.L. Ban, *Proc. R. Soc. Lond. A: Mat. Phys. Eng. Sci.* 327, 501-517 (1972).
15. J. Bauer, A. Schroer, R. Schwaiger, I. Tesari, C. Lange, L. Valdevit and O. Kraft, *Extreme Mechanics Letters* 3, 105-112 (2015).
16. M.A. Meyers and K.K. Chawla, *Mechanical Behavior of Materials*, 2nd ed. (Cambridge University Press, Cambridge, 2009) pp. 404-465.
17. H. Gao, B. Ji, I.L. Jäger, E. Arzt and P. Fratzl, *Proc. Natl. Acad. Sci. U.S.A.* 100, 5597-5600 (2003).
18. K. Kawamura and G.M. Jenkins, *J. Mater. Sci.* 7, 1099-1112 (1972).
19. R.E. Bullock and J.L. Kaae, *J. Mater. Sci.* 14, 920-930 (1979).
20. R. Schwaiger, M. Weber, B. Moser, P. Gumbsch and O. Kraft, *J. Mater. Res.* 27, 266-277 (2012).